Proteomic analysis demonstrated transcription factor *YRR1* gene deletion in *Saccharomyces cerevisiae* enhances its resistance to vanillin through the upregulation of transcriptional activator Haa1, coactivator Mbf1, and proteasome assembly chaperone Tma17 expression

Wenyan Cao
Qilu University of Technology
Xinning Wang (xnwang@qlu.edu.cn)
Qilu University of Technology https://orcid.org/0000-0002-3483-5300
Weiquan Zhao
Qilu University of Technology
Yu Shen
Shandong University
Wensheng Qin
Leakhead University
Zailu Li
Qilu University of Technology
Xiaoming Bao
Qilu University of technology

Research

Keywords: YRR1, quantitative proteomics, vanillin resistance, bioethanol, Saccharomyces cerevisiae

Posted Date: February 28th, 2020

DOI: https://doi.org/10.21203/rs.2.24803/v1

Abstract

Background: Vanillin is one of the major phenolic inhibitors in *Saccharomyces cerevisiae* for cellulosic ethanol production. Deleting transcription factor gene *YRR1* improves vanillin resistance by promoting some translation-related processes that were confirmed at the transcription level in our previous studies. However, the known genes regulated by Yrr1 are not related to translation process. Therefore, in this work, we investigated the effects of proteomic changes on vanillin stress and *YRR1* deletion to provide different perspectives from transcriptome analysis for comprehending the mechanisms of *YRR1* deletion in yeast protective response to vanillin.

Results: In wild-type cells, vanillin reduced the numbers of ribosomal proteins quantities and thereby inhibited cells' translation. *YRR1* deletion changed the quantities of 121 proteins which have no overlaps with transcriptomic changes. Of 112 proteins were up-regulated; 48 of 112 up-regulated proteins are involved in stress response, translational and basal transcriptional regulation. Fermentation data showed that the overexpression of *HAA1*, *MBF1*, and *TMA17*, which encode transcriptional activator, coactivator, and proteasome assembly chaperone, respectively, enhanced resistance to vanillin in *S. cerevisiae.*

Conclusions: These results showed how *YRR1* deletion increase vanillin resistance at protein level. This may advance our understanding of molecular mechanisms for *YRR1* deletion to protect yeast from vanillin stress and offer novel targets of genetic engineering for designing inhibitor-resistant ethanologenic yeast strains.

Background

Saccharomyces cerevisiae is a traditionally competitive cell factory for bioethanol and the production of other desired chemicals due to its superior robustness and its ease of genetic manipulation [1, 2]. Lignocellulosic materials have been viewed as a major resource for bioethanol production worldwide because they are massive, renewable, and do not compete with food resources [3]. However, the pretreatment of lignocellulose is inevitable to generate many inhibitors that hamper microorganism growth and fermentation, such as organic acid, furans, and phenolic compounds [4]. Vanillin, one of the major phenolic aldehyde compounds, has been considered a more effective repressor of ethanol fermentation than other lignocellulose-derived toxic compounds [5]. Thus, it is essential to understand the physiological mechanism of how vanillin inhibits S. cerevisiae growth and fermentation during the assembly of vanillin-resistant S. cerevisiae cell factories for bioethanol production.

In our previous work, we reported that the deletion of the multi-drug resistance-related transcription factor gene YRR1 remarkably improved S. cerevisiae vanillin resistance. The transcriptome analysis was initiated between the YRR1-deletion strain and the wild-type one either with or without vanillin stress. The outcome showed that vanillin repressed ribosome biogenesis and rRNA processing in the wild-type strain [6]. However, the deletion of YRR1 could prevent this repression. The genes related to ribosome biogenesis and rRNA processing are more up-regulated in the YRR1-deletion strain compared to the wild-

type under vanillin stress. Ribosomes and rRNA are vital for translation and protein synthesis [6]. Thus, YRR1 was considered to impact translation and protein synthesis. In addition, several studies have revealed that many inhibitors, including vanillin, furfural, 5- hydroxymethyl furfural (HMF), and acidic stress, repress translational initiation by blocking ribosome assembly, which leads to the accumulation of cytoplasmic processing bodies (P-bodies) and stress granules (SGs) [7–9].

Therefore, global mRNA profiles alone are not sufficient to present the changes in the biological system because translational, post-translational regulation mechanisms, protein degradation, and other events have not been taken into account. It is a common phenomenon that transcripts do mismatch with protein levels [10, 11].

Taken together, to gain a complete insight into the mechanism behind how YRR1 deletion protects yeast from vanillin stress, we conducted a quantitative proteomic analysis of yeast treated with specific vanillin stress and deleting YRR1, respectively. These proteomic data were analyzed in combination with previous transcriptome data obtained under the same conditions. This study demonstrated that when facing vanillin stress, S. cerevisiae cut down translation by reducing ribosomal proteins to save energy and promote energy production pathways for survival. The YRR1 deletion protective mechanism of vanillin resistance up-regulates proteins related to the stress response as well as basal transcriptional and translational regulation. The overexpression of three proteins (transcriptional activator Haa1, proteasome assembly chaperone Tma17 and transcriptional coactivator Mbf1) remarkably improved the resistance of yeast to vanillin. These results enriched the mechanism of the YRR1 deletion protective response to vanillin stress and offered novel strategies for genetic engineering manipulation to obtain high inhibitor-resistant microbes for second-generation fuel ethanol technology.

Results And Discussion

Quantitative proteomics reveals remarkable alterations in the protein abundance response to vanillin

To investigate the changes in protein abundance induced by vanillin stress perturbation, the proteomic differences were examined in the BY4741 laboratory strain in samples treated with and without vanillin. Based upon our stringent data mining criteria, a threshold of 1.3-fold was applied to filter out proteins that are differentially expressed. Among them, 135 proteins were up-regulated, and 83 proteins were down-regulated in response to vanillin (P-value < 0.05). Functional annotation of all the identified proteins was conducted based on the Gene Ontology (GO) database [12] and the Kyoto Encyclopedia of Genes and Genomes (KEGG) database [13]. The KEGG pathway enrichment of the different expressed proteins (DEPs) suggests that activated protein genes are mainly involved in the functional categories of energy production, amino acid metabolism and transport, the biosynthesis of secondary metabolites and others (Fig. 1a). In contrast, repressed protein genes are largely involved in the functional categories of ribosome, amino acid metabolism and biosynthesis of secondary metabolites (Fig. 1b).

Proteomes exhibited visible differences from transcriptomes in the presence of vanillin

Considering of the repression of the translation initiated by vanillin, mRNA most likely cannot represent a protein situation. Thus, the proteomic dataset was compared to data from a previous transcriptomic outcome (GEO accession number: GSE89854) to investigate the correlation between mRNA and protein levels [6]. Overlaps (i.e., homo-directional) between DEPs and differentially expressed genes (DEGs) are shown in the Venn diagrams (Fig. 2a). Only 23.8% of these DEPs exhibited a homo-directional change at the level of their transcript counterparts. A scatter plot was used to compare high-quality protein with the transcript expression ratios for all 218 DEPs (Fig. 2b). The positive Spearman rank correlation coefficient (Sr) of 0.47 that was calculated for these 218 DEPs revealed a weak correlation between transcriptome and proteome. This phenomenon is likely due to vanillin's ability to repress translation [7].

The DEPs and DEGs enriched ($p < 0.05$) in KEGG pathways are listed in Fig. 2c. Glycolysis-related genes/proteins and ABC transporters were up-regulated both at the mRNA and protein levels, which indicates that vanillin stimulates these two categories at the transcriptional level. Both the "pentose phosphate pathway (PPP)" and the "ribosome biogenesis pathway" were down-regulated only at the mRNA level. Ribosomal proteins and RNA polymerases were significantly decreased only at the protein level, which indicates that vanillin might repress the translation of the corresponding proteins or influence their post-transcriptional regulation.

Ribosomal proteins and rRNA processing-related proteins significantly decreased under vanillin stress

Although the transcriptome showed that 13 genes related to ribosome biogenesis were notably down-regulated (Table 1), the corresponding proteins exhibited no changes in protein abundance [6]. However, 20 ribosomal proteins were sharply suppressed by vanillin, including 5 small subunits of ribosomes (40S) and 15 large ribosomal subunits (60S) (Table 1). Moreover, one ribosome biogenesis-related protein (Rlp24) [14], three proteins (Esf1, Nsa2, Pop8) involved in rRNA processing, two RNA polymerase I subunits (Rpa12, Rpa190), one RNA polymerase III subunit (Rpc11), tRNA 4-demethylwyosine synthase Tyw1, and ATPase for tRNA processing Nbp35 also displayed a visible decrease in protein abundance. These down-regulated proteins were constituents of the cellular translational machine, which indicates that vanillin blocks translation efficiency and protein synthesis by reducing the quantity of ribosomal proteins available. This phenomenon coincided with the facts that vanillin inhibits translation initiation, so the cells do not need many more ribosomes. Therefore, the reduction of ribosome biogenesis is likely representative of the cell's effort to conserve energy for survival since ribosome biogenesis demands a great supply of energy [15, 16].

Table 1

Differentially expressed genes/proteins related to ribosomal proteins, ribosome biogenesis and rRNA processing in response to vanillin stress

ORF	Protein/gene	Description	DEPs Ratio[a] /DEGs log2 ratio[b]
Ribosomal proteins at protein level			DEPs Ratio
YDR025W	Rps11a	ribosomal 40S subunit protein S11A	0.724
YPR132W	Rps23b	ribosomal 40S subunit protein S23B	0.753
YLR388W	Rps29a	ribosomal 40S subunit protein S29A	0.660
YDL061C	Rps29b	ribosomal 40S subunit protein S29B	0.610
YNL096C	Rps7b	ribosomal 40S subunit protein S7B	0.763
YKL006W	Rpl14a	ribosomal 60S subunit protein L14A	0.695
YHL001W	Rpl14b	ribosomal 60S subunit protein L14B	0.709
YGR148C	Rpl24b	ribosomal 60S subunit protein L24B	0.727
YBL092W	Rpl32	ribosomal 60S subunit protein L32	0.755
YPL143W	Rpl33a	ribosomal 60S subunit protein L33A	0.656
YOR234C	Rpl33b	ribosomal 60S subunit protein L33B	0.644
YIL052C	Rpl34b	ribosomal 60S subunit protein L34B	0.707
YMR194W	Rpl36a	ribosomal 60S subunit protein L36A	0.752
YPL249C-A	Rpl36b	ribosomal 60S subunit protein L36B	0.743
YLR185W	Rpl37a	ribosomal 60S subunit protein L37A	0.740
YLR325C	Rpl38	ribosomal 60S subunit protein L38	0.719
YNL162W	Rpl42a	ribosomal 60S subunit protein L42A	0.765
YPR043W	Rpl43a	ribosomal 60S subunit protein L43A	0.700
YPL198W	Rpl7b	ribosomal 60S subunit protein L7B	0.683
YHL033C	Rpl8a	ribosomal 60S subunit protein L8A	0.746

[a] DEPs ratio (BY4741with/without vanillin stress) which is less than 1 means down-regulation at protein level.

[b] log2 ratio (BY4741with/without vanillin stress) which is less than 0 means down-regulation at mRNA level.

ORF	Protein/gene	Description	DEPs Ratio[a] /DEGs log2 ratio[b]
rRNA processing at protein level			
YDR365C	Esf1	Nucleolar protein involved in pre-rRNA processing	0.742
YBL018C	Pop8	ribonuclease P	0.750
YER126C	Nsa2	rRNA-processing protein NSA2	0.727
YDR279W	Rnh202	Ribonuclease H2 subunit	0.710
YJR063W	Rpa12	RNA polymerase I core subunit RPA12	0.750
YOR341W	Rpa190	RNA polymerase I core subunit RPA190	0.746
YDR045C	Rpc11	RNA polymerase III core subunit RPC11	0.730
YLR009W	Rlp24	ribosome biosynthesis protein	0.719
Ribosome biogenesis at mRNA level			DEGs log2 ratio
YOL077C	Brx1	ribosome biogenesis protein	-1.4
YAL025C	Mak16	ribosome biosynthesis protein	-1.2
YOL041C	Nop12	involved in biogenesis of large 60S ribosomal subunit	-1.3
YPL043W	Nop4	mRNA-binding ribosome biosynthesis protein	-1.0
YDR496C	Puf6	negative regulation of translation, ribosomal large subunit biogenesis	-1.5
YHR066W	Ssf1	rRNA-binding ribosome biosynthesis protein	-1.1
YPL226W	New1	ATP binding cassette protein	-1.1
YGR159C	Nsr1	required for pre-rRNA processing and ribosome biogenesis	-1.4
YDR398W	Utp5	Subunit of U3-containing Small Subunit processome complex	-1.0
YDR299W	Bfr2	rRNA-processing protein	-1.3
YNL112W	Dbp2	DEAD-box ATP-dependent RNA helicase	-1.5

[a] DEPs ratio (BY4741with/without vanillin stress) which is less than 1 means down-regulation at protein level.

[b] log2 ratio (BY4741with/without vanillin stress) which is less than 0 means down-regulation at mRNA level.

ORF	Protein/gene	Description	DEPs Ratio[a] /DEGs log2 ratio[b]
YAL025C	Mak16	ribosome biosynthesis protein	-1.2
YOL041C	Nop12	Nucleolar protein involved in pre-25S rRNA processing	-1.3
[a] DEPs ratio (BY4741with/without vanillin stress) which is less than 1 means down-regulation at protein level.			
[b] log2 ratio (BY4741with/without vanillin stress) which is less than 0 means down-regulation at mRNA level.			

Vanillin stress increased the quantity of proteins involved in energy generation

As shown in Table 2, a number of enzymes involved in energy generation pathways, such as glycolysis, oxidative phosphorylation, and the PPP, were dramatically up-regulated. Six glycolytic enzymes (Pyc1p, Tdh1, Tdh2, Hxk2, Eno1, and Gpm2) associated with glycolysis were remarkably increased. In particular, Hxk2, the predominant enzyme that catalyzes the first irreversible step of glycolysis [17], was up-regulated more than 1.5 times. Hxk2 is first of two rate-limiting enzymes in glycolysis [18]. Moreover, the proteins related to adenosine triphosphatase (ATP) synthesis, including the five ATP synthase subunits (Atp20, Atp7, Atp15, Atp14, and Tim11), three cytochrome c oxidase subunits (Cox4, Cox12, and Cox8), four ubiquinol cytochrome-c reductase subunits (Qcr9, Qcr2, Cor1, and Qcr6), and one ATPase (Pma2), also increased significantly. The up-regulated glycolysis and oxidative phosphorylation pathways tend to supply more ATP for cellular survival as the detoxification of vanillin consumes energy. For example, when facing vanillin stress, one strategy is to up-regulate some ATP binding cassette (ABC) transporters, such as Pdr5 and Snq2 (up-regulated 1.68 and 3.78 times, respectively, at the protein level), to extrude vanillin from the cells. These two transporters were also up-regulated at the mRNA level [6].

Table 2

Differentially expressed proteins related to energy metabolism in response to vanillin

ORF	Protein name	Description	DEPs Ratio[a]
ATP biosynthetic process			
YPR020W	Atp20	F1F0 ATP synthase subunit g	1.37
YKL016C	Atp7	F1F0 ATP synthase subunit d	1.33
YPL271W	Atp15	F1F0 ATP synthase subunit epsilon	1.43
YLR295C	Atp14	F1F0 ATP synthase subunit h	2.04
YPL036W	Pma2	H (+)-exporting P2-type ATPase	1.39
YDR322C-A	Tim11	F1F0 ATP synthase subunit e	1.35
electron transport and membrane-associated energy conservation			
YGR183C	Qcr9	ubiquinol-cytochrome-c reductase subunit 9	1.43
YPR191W	Qcr2	ubiquinol-cytochrome-reductase	1.33
YBL045C	Cor1	ubiquinol-cytochrome-reductase	1.34
YGL187C	Cox4	cytochrome c oxidase subunit IV	1.37
YLR038C	Cox12	cytochrome c oxidase subunit VIb	1.32
YFR033C	Qcr6	ubiquinol-cytochrome-c reductase subunit 6	1.31
YLR395C	Cox8	cytochrome c oxidase subunit VIII	1.38
Glycolysis/gluconeogenesis			
YGR254W	Eno1	phosphopyruvate hydratase ENO1	1.52
YJL052W	Tdh1	Glyceraldehyde-3-phosphate dehydrogenase	1.84
YGL253W	Hxk2	hexokinase 2	1.53
YDL021W	Gpm2	phosphoglycerate mutase family	1.41
YJR009C	Tdh2	Glyceraldehyde-3-phosphate dehydrogenase	1.69

[a] DEPs ratio (BY4741with/without vanillin stress) which is less than 1 means down-regulation.

Two enzymes (Gnd1 and Sol3) of the PPP increased over 1.5 times, especially the enzyme Gnd1, which generates nicotinamide adenine dinucleotide phosphate (NADPH) during its catalysis [19]. The PPP is the major source of NADPH, a vital cofactor for vanillin conversion to vanillyl alcohol, which is less toxic than vanillin [20, 21]. In the face of vanillin stress, another resistance strategy of S. cerevisiae is utilization of NADPH-dependent alcohol dehydrogenase (ADH) enzymes, such as Adh6/7, for vanillin transformation [22, 23].

ORF	Protein name	Description	DEPs Ratio[a]
YGL062W	Pyc1	pyruvate carboxylase 1	1.31
pentose-phosphate shunt, oxidative branch			
YHR183W	Gnd1	phosphogluconate dehydrogenase	1.64
YHR163W	Sol3	6-phosphogluconolactonase	1.51
[a] DEPs ratio (BY4741with/without vanillin stress) which is less than 1 means down-regulation.			
Two enzymes (Gnd1 and Sol3) of the PPP increased over 1.5 times, especially the enzyme Gnd1, which generates nicotinamide adenine dinucleotide phosphate (NADPH) during its catalysis [19]. The PPP is the major source of NADPH, a vital cofactor for vanillin conversion to vanillyl alcohol, which is less toxic than vanillin [20, 21]. In the face of vanillin stress, another resistance strategy of S. cerevisiae is utilization of NADPH-dependent alcohol dehydrogenase (ADH) enzymes, such as Adh6/7, for vanillin transformation [22, 23].			

Thus, the lower number of ribosomal proteins and ribosome biogenesis proteins to conserve energy as well as the higher level of glycolysis and oxidative phosphorylation pathway for producing more energy are thought to be an adaption of yeast for survival in response to vanillin stress.

Comparative proteomics analysis of the deletion of YRR1

Our previous study found that vanillin repressed ribosome biogenesis and pathways. In addition, the deletion of YRR1 could lower this repression and lead to improving resistance of S. cerevisiae to vanillin [6]. Thus, YRR1 was considered to be related to ribosome biogenesis or translation pathways. However, the known YRR1 targets are mostly related to ABC transporters and permeases, not the two aforementioned pathways. Further, the deletion of YRR1 triggered only eight genes (YBR230W-A, CAR2, FMP45, YCL048W-A, SCS3, UTH1, PMP3, and YIL002W-A), which have no effect on vanillin resistance expressed differently at the mRNA level (data not shown). To investigate the protein quantity changes caused by deleting YRR1, a proteomic analysis was conducted between BY4741(yrr1Δ) and BY4741. The outcome revealed that there were 121 DEPs, including 112 up-regulated and 9 down-regulated proteins that had no overlap with their corresponding mRNA level. The up-regulated DEPs were divided into functional categories according to the MIPS Functional Catalog and mainly felt in transcription, translation, and energy generation categories (Table 3). The functions of differentially expressed proteins are listed in Table 4.

Table 3

Functional classification of up-regulated proteins of YRR1 deletion

MIPS functional category	Number of genes in category	P-value
RNA transport	9	1×10^{-5}
transcriptional control	19	5×10^{-5}
energy generation	4	3×10^{-4}
electron transport	7	4×10^{-4}
rRNA processing	9	1×10^{-3}
RNA binding	9	3×10^{-3}
translation elongation	3	4×10^{-3}
translation termination	2	0.01
Significance was estimated with FunSpec (http://funspec.med.utoronto.ca/) based on the hypergeometric distribution of the MIPS functional categories of the differentially expressed proteins compared to the yeast proteome (P-value smaller than 0.01, bonferroni correction applied).		
The deletion of YRR1 stimulated quantity changes of translational proteins		
In the present proteomic data, a series of rRNA processing proteins were up-regulated after deleting YRR1. Among them, Nop6, Nhp2, Naf1, Lsm5, Nsr1, and Fyv7 participate in the synthesis of the 40S (small) ribosomal subunit. Cgr1 is involved in processing rRNA for the 60S ribosomal subunit [24]. The elements of rRNA synthesis also displayed increases, including the subunit of RNA polymerase I Rpa34, the RNA polymerase III assembly protein Rbs1, and two transcription factors (Hmo1 and Abf1) involved in activating rRNA and ribosomal protein transcription under the control of the TOR pathway [25–27]. Moreover, several regulators of translation, including three translation initiation factors (Tif11, Hcr1, and Gis2), were also up-regulated. Considering its ability to repress ribosome genesis and translation by vanillin stress, the deletion of YRR1 might strengthen translational elements to promote vanillin resistance in yeast.		
Intriguingly, three translational suppressors also increased, including two 4E-binding proteins, Caf20 and Eap1, which inhibit translational initiation by competing with translation initiation factor eIF4G to bind with eIF4E [28]. The other translational repressor was Stm1, which was previously demonstrated to repress translational elongation by limiting the interaction of elongation factor eEF3 with ribosomes and stalling ribosomes [29]. Further, one recent study indicated that Stm1 also worked as a ribosome preservation factor in response to nutrient stress and facilitated ribosomal protein synthesis rates once nutrients are restored [30]. These three proteins assist with the formation of P-bodies [31, 32]. P-bodies are viewed as reservoirs of mRNA after translation inhibition, and they are later released to reenter translation [33, 34]. It is likely that the absence of YRR1 can protect yeast cells against vanillin stress by promoting the formation of P-bodies to store translation elements and saving energy for the de-novo synthesis of translation machinery.		
The deletion of YRR1 promotes RNA polymerase II-directed transcription		

Table 4

Differentially expressed proteins induced by the deletion of YRR1

ORF	Protein	Description	DEPs ratio[a]
regulation of translation			
YOR276W	Caf20	Phosphoprotein of the mRNA cap-binding complex	1.64
YKL204W	Eap1	eIF4E-associated protein	1.39
YNL255C	Gis2	mRNA-binding translational activator	1.40
YCL037C	Sro9	RNA-binding protein	1.31
YHR087W	Rtc3	Protein of unknown function involved in RNA metabolism	1.43
YDR432W	Npl3	mRNA-binding protein promotes elongation, regulates termination	1.37
YDL053C	Pbp4	Pbp1p binding protein	1.39
YOL123W	HRP1	required for the cleavage and polyadenylation of pre-mRNA 3' ends	1.31
YLR150W	Stm1	Protein required for optimal translation under nutrient stress	1.42
rRNA processing			
YER146W	Lsm5	possibly involved in processing tRNA, snoRNA, and rRNA	1.31
YDL208W	Nhp2	snoRNA-binding protein NHP2 rRNA processing	1.42
YGL029W	Cgr1	Protein involved in processing of pre-rRNA	1.60
YGR159C	Nsr1	pre-rRNA processing and ribosome biogenesis	1.40
YLR192C	Hcr1	translation initiation factor eIF3 core subunit	1.43
YNL124W	Naf1	RNA-binding snoRNA assembly	1.67
YLR068W	Fyv7	Nucleolar protein required for maturation of 18S rRNA	1.36
transcription by RNA polymerase I			
YDR174W	Hmo1	Chromatin associated high mobility group	1.38
YMR263W	Sap30	Component of Rpd3L histone deacetylase complex	1.39
YER088C	Dot6	Protein involved in rRNA and ribosome biogenesis	1.37
YJL148W	Rpa34	RNA polymerase I subunit A34.5	1.47

[a] DEPs ratio (BY4741(yrr1Δ)/ BY4741) which is more than 1 means up-regulation.

ORF	Protein	Description	DEPs ratio[a]
YDL213C	Nop6	rRNA-binding protein required for 40S ribosomal subunit biogenesis	1.44
YMR260C	Tif11	Translation initiation factor eIF1A	1.36
nucleobase-containing compound transport			
YOR098C	Nup1	FG-nucleoporin NUP1	1.35
YLR335W	Nup2	FG-nucleoporin NUP2	1.43
YGR119C	Nup57	FG-nucleoporin NUP57	1.33
YJL041W	NSP1	FG-nucleoporin NSP1	1.55
microRNA biogenesis			
YDL189W	Rbs1	assembly of the RNA polymerase III complex	1.40
Transcription factor and cofactor			
YDR167W	Taf10	Subunit of TFIID and SAGA complexes	1.53
YLR399C	Bdf1	Protein involved in transcription initiation associates with the basal transcription factor TFIID	1.46
YKL112W	Abf1	DNA-binding protein ABF1	1.36
YPR133C	Spn1	Protein involved in RNA polymerase II transcription	1.35
YJR060W	Cbf1	Basic helix-loop-helix (bHLH) protein	1.57
YOR298C-A	Mbf1	Transcriptional coactivator transcription by RNA polymerase II	1.47
YER159C	Bur6	negative cofactor 2 transcription regulator complex subunit BUR6	1.38
YBR089C-A	Nhp6B	high-mobility group nucleosome-binding protein	1.47
YGL025C	Pgd1	Subunit of the RNA polymerase II mediator complex essential for basal and activated transcription	1.38
Transcription process regulation			
YML094W	Gim5	facilitates transcriptional elongation	1.43
YLR200W	Yke2	facilitates transcriptional elongation	1.53
Stress response			

[a] DEPs ratio (BY4741(yrr1Δ)/ BY4741) which is more than 1 means up-regulation.

ORF	Protein	Description	DEPs ratio[a]
YLR150W	Stm1	Protein required for optimal translation under nutrient stress	1.42
YML007W	Yap1	DNA-binding transcription factor YAP1	1.60
YPR008W	Haa1	Transcriptional activator involved in adaptation to weak acid stress	1.57
YNL027W	Crz1	Transcription factor, activates transcription of stress response genes	1.75
YMR074C	Sod2	superoxide dismutase	1.32
YJR104C	Sod1	superoxide dismutase	1.39
YDL110C	Tma17	ATPase dedicated chaperone that adapts proteasome assembly to stress;	1.59
YBL051C	Pin4	Protein involved in G2/M phase progression and response to DNA damage	1.49
YKL054C	Def1	DNA damage-responsive RNA polymerase-degradation factor DEF1	1.65
YFL014W	Hsp12	lipid-binding protein HSP12, induced by heat shock, oxidative stress	1.64

[a] DEPs ratio (BY4741(yrr1Δ)/ BY4741) which is more than 1 means up-regulation.

Arbitrary extracellular and intracellular stimulation can trigger a global adaptive transcriptional regulatory program in yeast cells. The deletion of YRR1 up-regulated several basal transcription factors (Taf10, Mbf1, Nhp6b, and Pgd1). These factors assist in recognizing promoters that contain a TATA box and assembly of the transcription preinitiation complex and thereby promote transcription of TATA-containing genes [35–38]. TATA-containing genes tend to be stress-responsive [39, 40]. Moreover, four transcription elongation factors (Gim5, Yke2, Spn1, and Npl3) also increased in conditions of protein abundance. Npl3, an mRNA-binding protein, is a positive transcription elongation factor shown to interact with the carboxy terminal domain (CTD) and have a direct stimulatory effect on the elongation activity of the polymerase [41]. Therefore, these results indicate that the deletion of YRR1 promotes TATA-containing gene transcription by the promotion of basal transcription factors to improve survival under vanillin stress.

The deletion of YRR1 improved S. cerevisiae's resistance to vanillin by increasing Tma17, Mbf1, and Haa1 at the protein level

The results of above proteomic analysis led us to investigate possible novel mechanisms between the deletion of YRR1 and a vanillin-tolerant phenotype. First, two proteins attracted our attention since they exhibited reverse variation in two proteomes: Rtc3, which is involved in RNA metabolism, and plasma membrane protein Hsp12, which plays a role in maintaining membrane organization. They were both

down-regulated by vanillin stress but up-regulated by YRR1 deletion. Their reverse variation is likely the reason why YRR1 deletion promotes the resistance of yeast to vanillin stress. However, the overexpression of these proteins had no effect on vanillin resistance (data not shown).

We investigated several up-regulated proteins that were associated with transcription and the stress response in a YRR1-deletion strain as candidates. These candidates were six stress response-related proteins (Crz1, Dsk2, Hsp12, Haa1, Def1, and Tma17) and four transcription-related proteins (Taf10, Mbf1, Gis2, and Tif11). To test these proteins'/genes' function in a vanillin-resistant phenotype, these genes were overexpressed in BY4741. The overexpression of HAA1, TMA17, and MBF1 enhanced the strain growth under vanillin stress (Fig. 3 and Fig. 4). The maximum specific growth rates of the transformants of HAA1, TMA17, and MBF1 were 18%, 33%, and 15% faster than the control in the presence of 6 mM vanillin, respectively (Table 5). The specific consumption rates for vanillin of strains overexpressing HAA1, TMA17, and MBF1 were 0.041, 0.041, and 0.029 g g^{-1} h^{-1}, respectively. Compared to the 0.034 g g^{-1} h^{-1} of the control (Table 5), only HAA1 and TMA17 significantly increased the specific vanillin consumption rates. MBF1 accelerated growth more than vanillin reduction. However, other genes related to translation did not significantly improve vanillin resistance (data not shown).

Table 5
Maximum specific growth rate and specific consumption rate for vanillin of recombinant strains

Strains	SD medium	SD with 6 mM vanillin	
	μ_{max} (h^{-1})	μ_{max} (h^{-1})	specific consumption rate for vanillin (g g^{-1} h^{-1})
BY4741(pJFE3)	0.273 ± 0.008	0.087 ± 0.005	0.034 ± 0.003
BY4741(HAA1)	0.252 ± 0.007	0.109 ± 0.002	0.041 ± 0.003
BY4741(TMA17)	0.280 ± 0.008	0.117 ± 0.002	0.041 ± 0.004
BY4741(MBF1)	0.116 ± 0.007	0.097 ± 0.005	0.029 ± 0.004

Haa1 is a critical transcription factor involved in the acid stress adaption of yeast cells [42]. It also contributes to vanillin resistance, which indicates that vanillin and acid stress share some common features, such as stimulating reactive oxygen species accumulation and inhibiting translation [7, 9, 43, 44]. Mbf1 is a transcriptional coactivator that mediates transcriptional activation by bridging the DNA-binding region of the activator and TBP (TATA binding protein) [45]. As mentioned above, TATA-containing genes are mainly associated with stress responses. Therefore, it was expected that Mbf1 could improve S. cerevisiae vanillin resistance by facilitating stress-response gene transcription. Under stress conditions, Tma17 (also named as Adc17) is the most important chaperone for yeast cellular

proteasome biogenesis and assembly. The deletion of TMA17 aggravates proteasome defects and reduced the cells' fitness. The maintenance of adequately functional proteasomes is vital for cells and organisms to adapt to changes and survive in their environment [46]. Thus, the deletion of YRR1 stimulated greater Tma17 expression to allow cells to adapt to vanillin stress better. These results suggested that the deletion of YRR1 could up-regulate HAA1, TMA17, and MBF1 at the protein level to enhance vanillin resistance.

Conclusions

This work investigated the changes in general protein composition induced by vanillin stress via quantitative proteome. The results indicated that S. cerevisiae adapted to vanillin stress by repressing ribosomal protein abundance and enhancing energy production. YRR1 deletion up-regulated proteins related to stress response, transcriptional and translational regulation, which provide different perspectives from transcriptome for comprehending the mechanisms behind the YRR1 deletion protective response in yeast. The finding that three proteins (Haa1, Tma17, and Mbf1) could enhance vanillin resistance by their overexpression will provide novel strategies for designing inhibitor-resistant ethanologenic yeast strains for bioethanol production.

Methods

Strains, plasmids, and medium

Wild-type *S. cerevisiae* strain BY4741 (*MATa, his3Δ1, leu2Δ0, met15Δ0, ura3Δ0*) and the *YRR1* deletion strain BY4741(*yrr1Δ*) (BY4741 derivate; *yrr1::loxP*) [6] that were previously stored and constructed in our laboratory, respectively. Any overexpressed genes were amplified from the genome of BY4741 with cutting sites and inserted into pJFE3, a 2-μ plasmid with the *TEF1* promoter, the *PGK1* terminator, and *URA3* as the selection marker [47]. Next, the resulting recombinant plasmids were transformed into BY4741.

Synthetic complete medium (SD) or Sc-URA medium (5 g L^{-1} ammonium sulfate, Sangon, China, 1.7 g L^{-1} yeast nitrogen base without amino acids, Sangon, China, CSM or CSM-URA, MP Biomedicals, Solon, OH, USA) was used for activation, batch fermentation, and protein sample preparation of recombinant strains by adding 20 g L^{-1} glucose. Vanillin was added to the medium as indicated. All of the cultures were incubated at 30°C.

Protein sample preparation for proteomic analysis

Yeast cells of BY4741 and BY4741(*yrr1Δ*) were harvested during the exponential growth phase (OD_{600}=1.6–2.0) in SD medium with or without of 5 mM vanillin, respectively. All of the proteomic analyses were carried out in biological triplicate. The sample was ground by liquid nitrogen into cell powder and then transferred to a 5-mL centrifuge tube. Four volumes of lysis buffer (8 M urea, 1%

protease inhibitor cocktail) were added to the cell powder, followed by sonication three times on ice using a high-intensity ultrasonic processor. The remaining debris was removed by centrifugation at 12,000 g for 10 min at 4°C. Finally, the supernatant was collected, and the protein concentration was determined using a BCA kit according to the manufacturer's instructions. For digestion, the protein solution was reduced with 5 mM dithiothreitol for 30 min at 56°C and alkylated with 11-mM iodoacetamide for 15 min at room temperature in darkness. The protein sample was then diluted by adding 100 mM TEAB to reduce the urea concentration to < 2 M. Finally, trypsin was added at a 1:50 trypsin-to-protein mass ratio for the first digestion overnight; the second 4-h digestion process had a 1:100 trypsin-to-protein mass ratio. A peptide of trypsin digestion was labeled with TMT, according to the manufacturer's protocol for a TMT kit.

High-performance liquid chromatography fractionation and mass spectrometric analysis

The labeling peptides were fractionated by high pH reverse-phase high-performance liquid chromatography (HPLC) using an Agilent 300 Extend C18 column (5-μm particles, 4.6 mm ID, 250 mm length). Briefly, the peptides were first separated into 60 fractions with a gradient ranging from 8–32% acetonitrile (pH 9.0) over 60 min. Then, the peptides were combined into 18 fractions and dried by vacuum centrifugation. The tryptic peptides were dissolved in solvent A (0.1% formic acid and 2% acetonitrile); the gradient was comprised of an increase from 6% to 20% solvent B (0.1% formic acid in 90% acetonitrile) over 20 min, from 20% to 33% in 11 min, and up to 80% in 4 min then holding at 80% for the last 3 min, all at a constant flow rate of 320 nL/min on an EASY-nLC 1000 UPLC system. The peptides were subjected to an NSI source followed by tandem mass spectrometry (MS/MS) in a Q Exactive^{TM} Plus (Thermo) coupled online to the UPLC. The electrospray voltage applied was 2.0 kV. The m/z scan range was 350–1800 for a full scan, and intact peptides were detected in the Orbitrap at a resolution of 70,000. The secondary mass spectrometry scan range was set as a fixed first point of 100 m/z, and the resolution was 17,500. The data acquisition mode was a data-dependent scanning (DDA) program; the first 20 peptides with the highest signal intensity are selected to enter the HCD collision cell, and then 30% of the fragmentation energy is used for fragmentation after the first-stage scanning; the same step performed once more during the secondary mass spectrometry analysis. To improve the effective utilization of the mass spectrometer, the automatic gain control (AGC) is set as 5E4, the signal threshold is set as 1E4, and the maximum injection time is set as 200 ms with 30 seconds of dynamic exclusion time.

Database searching and data analysis

The resulting MS/MS data were processed using the Maxquant search engine (v.1.5.2.8). Trypsin/P was specified as the cleavage enzyme and allowed up to two missing cleavages. The mass resistance for precursor ions was set as 20 ppm in the first search and 5 ppm in the main search, and the mass resistance for fragment ions was set as 0.02 Da. Carbamidomethyl on Cys was specified as a fixed modification, and oxidation on Met was specified as a variable modification. The method used to obtain relative protein expression ratios was set as TMT-6plex, and the FDR for protein identification and PSM identification was 1%. Proteins were classified into functional categories by GO annotation from the

Uniprot-GOA database (www. http://www.ebi.ac.uk/GOA/). Some undetermined proteins were identified using protein sequence-based algorithm software (InterProScan) to predict the GO function of the protein. Pathway enrichment analyses were carried out using the Kyoto Encyclopedia of Genes and Genomes (KEGG) database, and the subcellular location of the proteins was determined using software WoLF PSORT. The function of representative proteins was estimated using the MIPS Functional Catalogue database (http://funspec.med.utoronto.ca/, *P*-value < 0.01, Bonferroni correction). To explore the relationship between the proteome and the transcriptome, the relation of them was contrasted and verified by utilizing the Statistical Package for the Social Sciences (SPSS) software (Spearman's correlation analysis), and their overlap was displayed in a Venn diagram using a bioinformatic tool(http://bioinformatics.psb.ugent.be/webtools/Venn/).

Fermentation

A single colony was precultured in 3 mL SC-URA at 30°C for 24 h. Then the cultures were transferred into 10 mL fresh medium with an initial OD_{600} at 0.2 and cultured overnight. Next, the cells were inoculated into 100-mL flasks containing 40 mL fermentation medium in the presence or absence of 6 mM vanillin with an initial OD_{600} of 0.2. The fermentation was carried out at 30°C and 200 rpm.

Analyses of extracellular vanillin

The concentrations of vanillin and vanillyl alcohol were determined by HPLC Waters e2695 (Waters, USA) equipped with an Xbridge^{TM}-C18 column (Waters, USA). The peaks were detected at room temperature using ultraviolet detection (PDA-2998) at 210 nm with a mobile phase containing 40% absolute methanol (Chromatographic grade, Fisher Chemical, USA) supplied at a flow rate of 0.6 mL min^{-1}[6].

Analyses of Physiological Parameters

The biomass concentrates were investigated to determine their correlation with OD_{600} and the dry cell weight (DCW). Different strains exhibited different coefficients between OD_{600} and the DCW (data not shown). The maximum growth rates were regarded as the linear regression coefficients of the ln (OD_{600}) versus time during the exponential growth phase. Specific consumption rates of vanillin were calculated as previously described [48].

Abbreviations

HMF
hydroxymethyl furfural; P-bodies:processing bodies; SGs:stress granules; HPLC:high-performance liquid chromatography; DDA:data-dependent scanning; AGC:automatic gain control; KEGG:Kyoto Encyclopedia of Genes and Genomes; SPSS:Social Sciences software; DCW:dry cell weight; GO:Gene Ontology; DEPs:different expressed proteins; DEGs:differentially expressed genes; Sr:Spearman rank; PPP:pentose phosphate pathway; ATP:adenosine triphosphatase; ABC:ATP binding cassette; NADPH:nicotinamide adenine dinucleotide phosphate; ADH:alcohol dehydrogenase.

Declarations

Ethics approval and consent to participate

Not applicable.

Consent for publication

Not applicable.

Availability of data and materials

The datasets used and/or analysed during the current study are available from the corresponding author on reasonable request.

Competing interests

The authors declare that they have no competing interests.

Funding

This work was supported by the National Key R&D Program of China (2018YFB1501401), the National Natural Science Foundation of China (31870063), the Shandong Provincial Natural Science Foundation (ZR2019BC080), the Key R&D Project of Shandong Province (2019JZZY010906), the Major Program of Shandong Province Natural Science Foundation (No. ZR2018ZB0209), the Special Funds for International Cooperative Research of Qilu University of Technology (Shandong Academy of Sciences) (QLUTGJHZ2018009), and the Foundation (No. ZZ20190306) of State Key Laboratory of Biobased Material and Green Papermaking, Qilu University of Technology, Shandong Academy of Sciences.

Authors' contributions

XW and WC conceived and designed the study and experiments; WC performed proteomic data analysis; WC and WZ conducted the experiments and collected data. XW and WC analyzed data and drafted the manuscript. XB, WQ, YS and ZL supervised and coordinated the overall study. All authors read and approved the final manuscript.

Acknowledgements

Not applicable.

Authors' details

[1]School of Biotechnology, Qilu University of Technology, Shandong Academy of Sciences, Jinan, 250353, China.

[2]State Key Laboratory of Biobased Material and Green Papermaking, Qilu University of Technology, Shandong Academy of Sciences, Jinan, 250353, China.

[3]State Key Laboratory of Microbial Technology, Institute of Microbial Technology, Shandong University, Binhai Road 72, Qingdao, 266237, China.

[4]Department of Biology, Lakehead University, 955 Oliver Rd, Thunder Bay, ON, P7B 5E1, Canada.

References

1. Gibson BR, Lawrence SJ, Leclaire JPR, Powell CD, Smart KA. Yeast responses to stresses associated with industrial brewery handling. FEMS Microbiol Rev. 2007; 31:535-569.
2. Hong K-K, Nielsen J. Metabolic engineering of *Saccharomyces cerevisiae*: a key cell factory platform for future biorefineries. Cell Mol Life Sci. 2012; 69:2671-2690.
3. Kim S, Dale BEJB, bioenergy. Global potential bioethanol production from wasted crops and crop residues. Biomass Bioenergy. 2004; 26:361-375.
4. Saini JK, Saini R, Tewari L. Lignocellulosic agriculture wastes as biomass feedstocks for second-generation bioethanol production: concepts and recent developments. 3 Biotech. 2015; 5:337-353.
5. Klinke HB, Thomsen AB, Ahring BK. Inhibition of ethanol-producing yeast and bacteria by degradation products produced during pre-treatment of biomass. Appl Microbiol Biot. 2004; 66:10-26.
6. Wang X, Liang Z, Hou J, Shen Y, Bao X. The absence of the transcription factor Yrr1p, identified from comparative genome profiling, increased vanillin tolerance due to enhancements of ABC transporters expressing, rRNA processing and ribosome biogenesis in *Saccharomyces cerevisiae*. Front Microbiol. 2017; 8:367.
7. Iwaki A, Ohnuki S, Suga Y, Izawa S, Ohya Y. Vanillin inhibits translation and induces messenger ribonucleoprotein (mRNP) granule formation in *saccharomyces cerevisiae*: application and validation of high-content, image-based profiling. PLoS One. 2013; 8:e61748.
8. Iwaki A, Kawai T, Yamamoto Y, Izawa SJAEM. Biomass conversion inhibitors furfural and 5-hydroxymethylfurfural induce formation of messenger RNP granules and attenuate translation activity in Saccharomyces cerevisiae. Appl Environ Microb. 2013; 79:1661-1667.
9. Iwaki A, Izawa S. Acidic stress induces the formation of P-bodies, but not stress granules, with mild attenuation of bulk translation in *Saccharomyces cerevisiae*. Biochem J. 2012; 446:225-233.
10. Vogel C, Marcotte EMJNrg. Insights into the regulation of protein abundance from proteomic and transcriptomic analyses. Nat Rev Genet. 2012; 13:227-232.
11. De Groot MJ, Daran-Lapujade P, van Breukelen B, Knijnenburg TA, de Hulster EA, Reinders MJ, Pronk JT, Heck AJ, Slijper M. Quantitative proteomics and transcriptomics of anaerobic and aerobic yeast cultures reveals post-transcriptional regulation of key cellular processes. Microbiology. 2007; 153:3864-3878.

12. The Gene Ontology C. The gene ontology resource: 20 years and still GOing strong. Nucleic Acids Res. 2019; 47:D330-D338.
13. Kanehisa M, Furumichi M, Tanabe M, Sato Y, Morishima KJNar. KEGG: new perspectives on genomes, pathways, diseases and drugs. Nucleic Acids Res. 2017; 45:D353-D361.
14. Gerhardy S, Menet AM, Peña C, Petkowski JJ, Panse VGJC. Assembly and nuclear export of pre-ribosomal particles in budding yeast. Chromosoma. 2014; 123:327-344.
15. Warner JRJTibs. The economics of ribosome biosynthesis in yeast. Trends Biochem Sci. 1999; 24:437-440.
16. Albert B, Kos-Braun IC, Henras AK, Dez C, Rueda MP, Zhang X, Gadal O, Kos M, Shore DJE. A ribosome assembly stress response regulates transcription to maintain proteome homeostasis. Elife. 2019; 8:e45002.
17. Bianconi ML. Calorimetric determination of thermodynamic parameters of reaction reveals different enthalpic compensations of the yeast hexokinase isozymes. J Biol Chem. 2003; 278:18709-18713.
18. Randez-Gil F, Sanz P, Entian K-D, Prieto JA. Carbon Source-Dependent Phosphorylation of Hexokinase PII and Its Role in the Glucose-Signaling Response in Yeast. Mol Cell Biol. 1998; 18:2940-2948.
19. Sinha A, Maitra PKJM. Induction of specific enzymes of the oxidative pentose phosphate pathway by glucono-δ-lactone in *Saccharomyces cerevisiae*. Microbiology. 1992; 138:1865-1873.
20. Cunha JT, Aguiar TQ, Romani A, Oliveira C, Domingues L. Contribution of *PRS3*, *RPB4* and *ZWF1* to the resistance of industrial *Saccharomyces cerevisiae* CCUG53310 and PE-2 strains to lignocellulosic hydrolysate-derived inhibitors. Bioresour Technol. 2015; 191:7-16.
21. Liu ZL. Molecular mechanisms of yeast tolerance and in situ detoxification of lignocellulose hydrolysates. Appl Microbiol Biotechnol. 2011; 90:809-825.
22. Wang X, Liang Z, Hou J, Bao X, Shen Y. Identification and functional evaluation of the reductases and dehydrogenases from *Saccharomyces cerevisiae* involved in vanillin resistance. BMC Biotechnol. 2016; 16:31.
23. Shen Y, Li H, Wang X, Zhang X, Hou J, Wang L, Gao N, Bao XJJoim, biotechnology. High vanillin tolerance of an evolved *Saccharomyces cerevisiae* strain owing to its enhanced vanillin reduction and antioxidative capacity. J Ind Microbiol Biotechnol. 2014; 41:1637-1645.
24. Moy TI, Boettner D, Rhodes JC, Silver PA, Askew DSJM. Identification of a role for *Saccharomyces cerevisiae* Cgr1p in pre-rRNA processing and 60S ribosome subunit synthesis. Microbiology. 2002; 148:1081-1090.
25. Berger AB, Decourty L, Badis G, Nehrbass U, Jacquier A, Gadal OJM, biology c. Hmo1 is required for TOR-dependent regulation of ribosomal protein gene transcription. Mol Cell Biol. 2007; 27:8015-8026.
26. Oliveira AP, Ludwig C, Zampieri M, Weisser H, Aebersold R, Sauer UJSS. Dynamic phosphoproteomics reveals TORC1-dependent regulation of yeast nucleotide and amino acid biosynthesis. Sci Signal. 2015; 8:rs4-rs4.

27. Fermi B, Bosio MC, Dieci GJCg. Multiple roles of the general regulatory factor Abf1 in yeast ribosome biogenesis. Curr Genet. 2017; 63:65-68.
28. Castelli LM, Talavera D, Kershaw CJ, Mohammad-Qureshi SS, Costello JL, Rowe W, Sims PF, Grant CM, Hubbard SJ, Ashe MPJPg. The 4E-BP Caf20p mediates both eIF4E-dependent and independent repression of translation. PLoS genetics. 2015; 11.
29. Balagopal V, Parker RJR. Stm1 modulates translation after 80S formation in *Saccharomyces cerevisiae*. RNA. 2011; 17:835-842.
30. Hayashi H, Nagai R, Abe T, Wada M, Ito K, Takeuchi-Tomita NJTJoB. Tight interaction of eEF2 in the presence of Stm1 on ribosome. J Biochem. 2018; 163:177-185.
31. Park K, Lee Y-S, Jung D, Kim JJJoM. Roles of eIF4E-binding protein Caf20 in Ste12 translation and P-body formation in yeast. J Microbiol. 2018; 56:744-747.
32. Balagopal V, Parker RJG. Stm1 modulates mRNA decay and Dhh1 function in *Saccharomyces cerevisiae*. Genetics. 2009; 181:93-103.
33. Brengues M, Teixeira D, Parker RJS. Movement of eukaryotic mRNAs between polysomes and cytoplasmic processing bodies. Science. 2005; 310:486-489.
34. Standart N, Weil DJTiG. P-bodies: cytosolic droplets for coordinated mRNA storage. Trends Genet. 2018; 34:612-626.
35. Matangkasombut O, Buratowski RM, Swilling NW, Buratowski SJG, Development. Bromodomain factor 1 corresponds to a missing piece of yeast TFIID. Gene Dev. 2000; 14:951-962.
36. Robinson PJ, Trnka MJ, Bushnell DA, Davis RE, Mattei P-J, Burlingame AL, Kornberg RDJC. Structure of a complete mediator-RNA polymerase II pre-initiation complex. Cell. 2016; 166:1411-1422. e1416.
37. Han Y, Luo J, Ranish J, Hahn SJTEj. Architecture of the *Saccharomyces cerevisiae* SAGA transcription coactivator complex. EMBO J. 2014; 33:2534-2546.
38. Sermwittayawong D, Tan SJTEj. SAGA binds TBP via its Spt8 subunit in competition with DNA: implications for TBP recruitment. EMBO J. 2006; 25:3791-3800.
39. López-Maury L, Marguerat S, Bähler JJNRG. Tuning gene expression to changing environments: from rapid responses to evolutionary adaptation. Nat Rev Genet. 2008; 9:583-593.
40. Bae S-H, Han HW, Moon JJPO. Functional analysis of the molecular interactions of TATA box-containing genes and essential genes. PLoS One. 2015; 10.
41. Dermody JL, Dreyfuss JM, Villén J, Ogundipe B, Gygi SP, Park PJ, Ponticelli AS, Moore CL, Buratowski S, Bucheli MEJPo. Unphosphorylated SR-like protein Npl3 stimulates RNA polymerase II elongation. PloS One. 2008; 3.
42. Swinnen S, Henriques SF, Shrestha R, Ho P-W, Sá-Correia I, Nevoigt EJMcf. Improvement of yeast tolerance to acetic acid through Haa1 transcription factor engineering: towards the underlying mechanisms. Microb Cell Fact. 2017; 16:7.
43. Giannattasio S, Guaragnella N, Zdralevic M, Marra E. Molecular mechanisms of *Saccharomyces cerevisiae* stress adaptation and programmed cell death in response to acetic acid. Front Microbiol.

2013; 4:33.

44. Nguyen TTM, Iwaki A, Ohya Y, Izawa S. Vanillin causes the activation of Yap1 and mitochondrial fragmentation in *Saccharomyces cerevisiae*. J Biosci Bioeng. 2014; 117:33-38.
45. Liu Q-X, Nakashima-Kamimura N, Ikeo K, Hirose S, Gojobori TJMb, evolution. Compensatory Change of Interacting Amino Acids in the Coevolution of Transcriptional Coactivator *MBF1* and TATA-Box–Binding Protein. Mol Biol Evol. 2007; 24:1458-1463.
46. Hanssum A, Zhong Z, Rousseau A, Krzyzosiak A, Sigurdardottir A, Bertolotti A. An inducible chaperone adapts proteasome assembly to stress. Mol Cell. 2014; 55:566-577.
47. Shen Y, Chen X, Peng BY, Chen LY, Hou J, Bao XM. An efficient xylose-fermenting recombinant *Saccharomyces cerevisiae* strain obtained through adaptive evolution and its global transcription profile. Appl Microbiol Biot. 2012; 96:1079-1091.
48. Peng B, Shen Y, Li X, Chen X, Hou J, Bao X. Improvement of xylose fermentation in respiratory-deficient xylose-fermenting *Saccharomyces cerevisiae*. Metab Eng. 2012; 14:9-18.

Figures

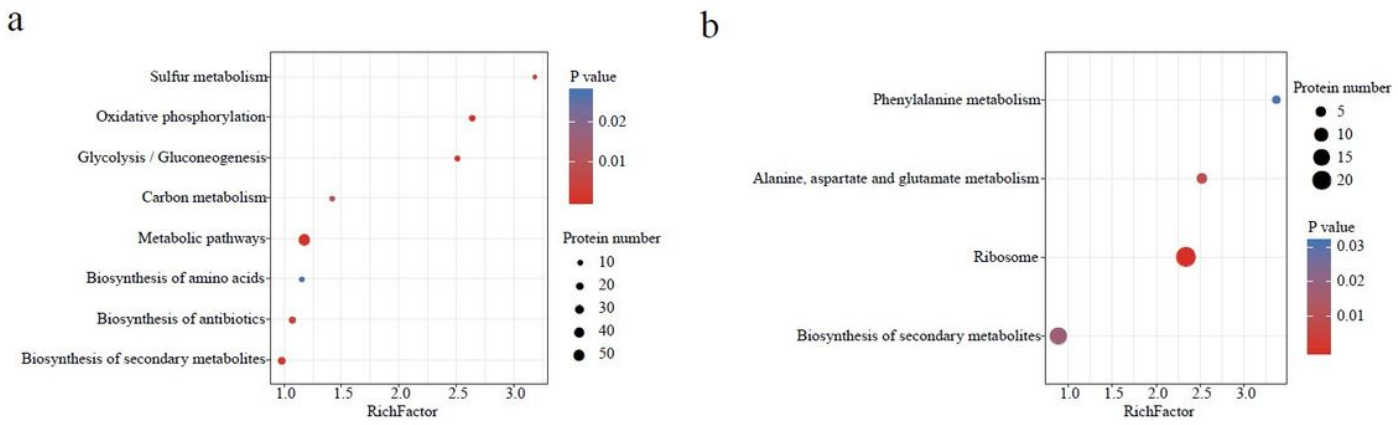

Figure 1

Statistics of KEGG pathway enrichment of DEPs of BY4741 response to BY4741 to vanillin. a) up-regulated proteins; b) down-regulated proteins. RichFactor is the ratio of DEP number annotated in this pathway term to all protein numbers annotated in this pathway term. Greater RichFactor indicates a greater effect of vanillin on the analyzed pathway.

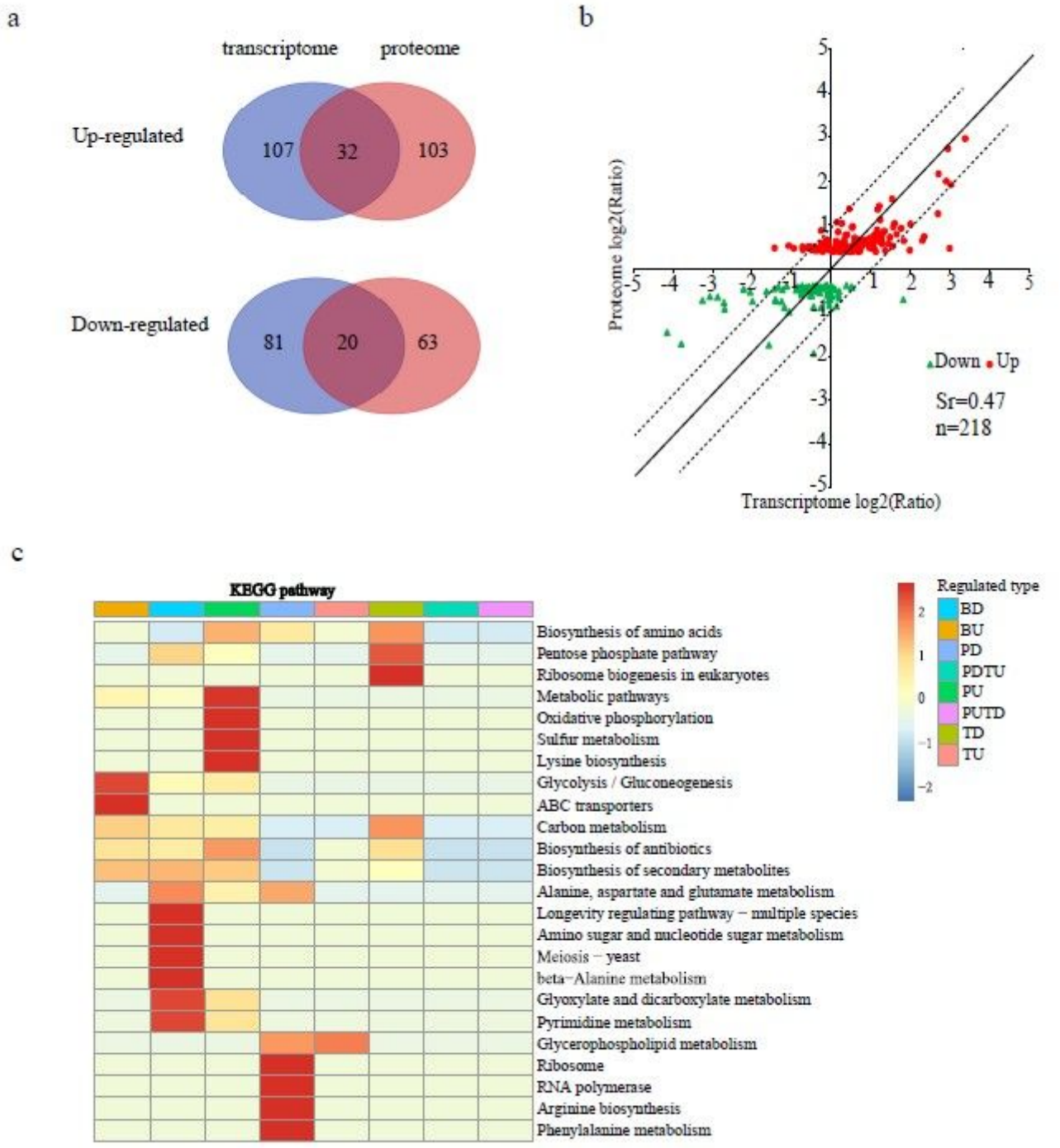

Figure 2

Proteomic analysis integrated with transcriptomics data of BY4741 under vanillin stress. a) The Venn diagram shows the overlaps of the transcriptomes and proteomes; b) A scatter plot of differently expressed protein (n=218) ratios versus the corresponding mRNA expression ratios. The plotted x=y line indicates data points showing a perfect correlation between mRNA and proteins. Dashed lines indicate a two-fold deviation between the mRNA and protein expression ratios. The greater the absolute value of Sr (Spearman), the stronger the correlation; c) The heatmap of the cluster analysis of differently expressed genes/proteins: BD and BU (both of protein and mRNA are down-regulated or up-regulated); PU and PD

(only up-regulated or down-regulated at protein level); TU and TD (only up-regulated or down-regulated at the mRNA level); PDTU (down-regulated at protein level and up-regulated at mRNA level); PUTD (up-regulated at protein level and down-regulated at mRNA level); Red indicates strong enrichment, and blue indicates weak enrichment.

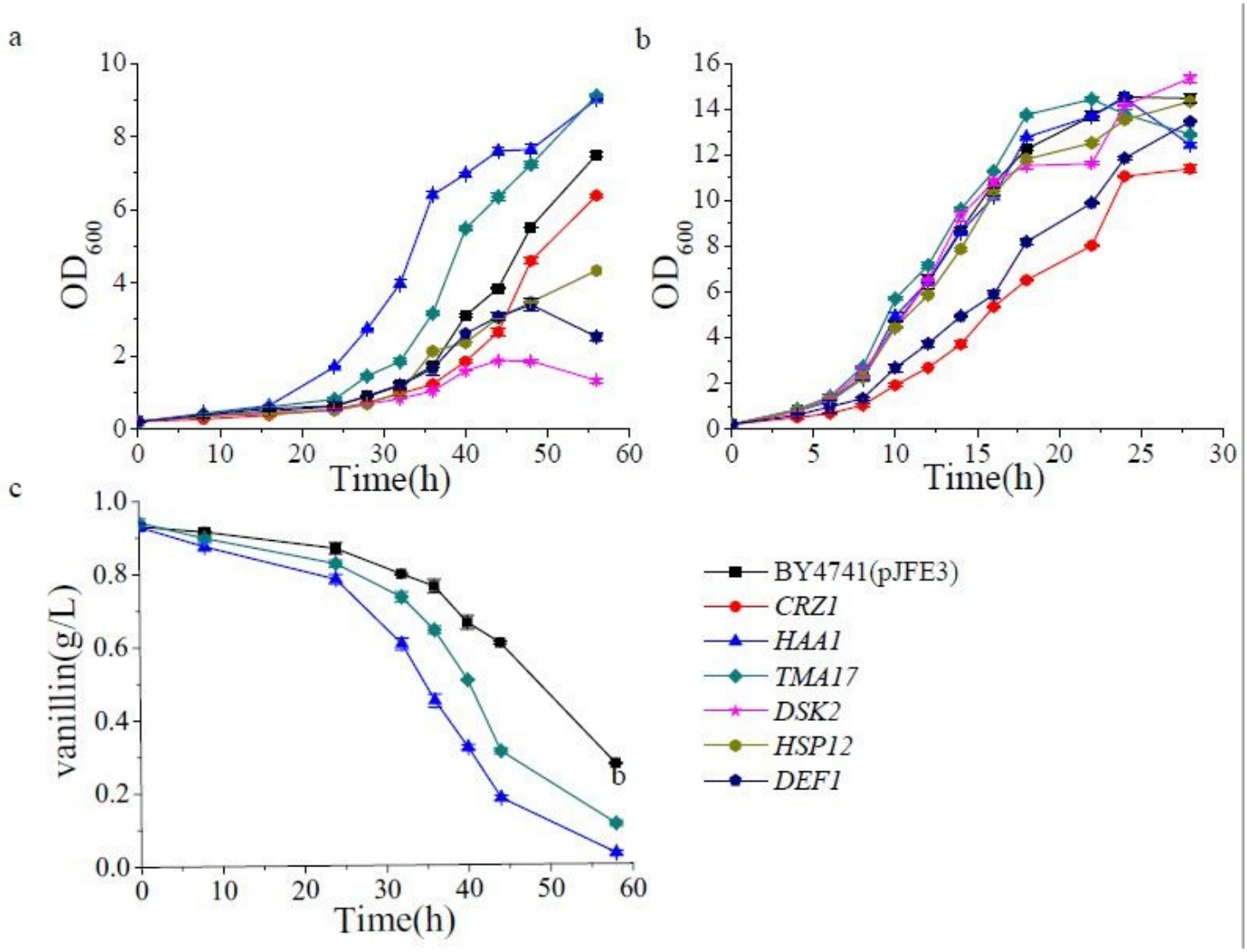

Figure 3

Vanillin resistance profiles of recombinant strains in Sc-URA liquid medium. The curve of growth under 6 mM vanillin stress (a) and without vanillin stress (b); the curve of vanillin reduction (c); BY4741(pJFE3) is the control. Data are the mean ± standard deviation of independent triplicate experiments.

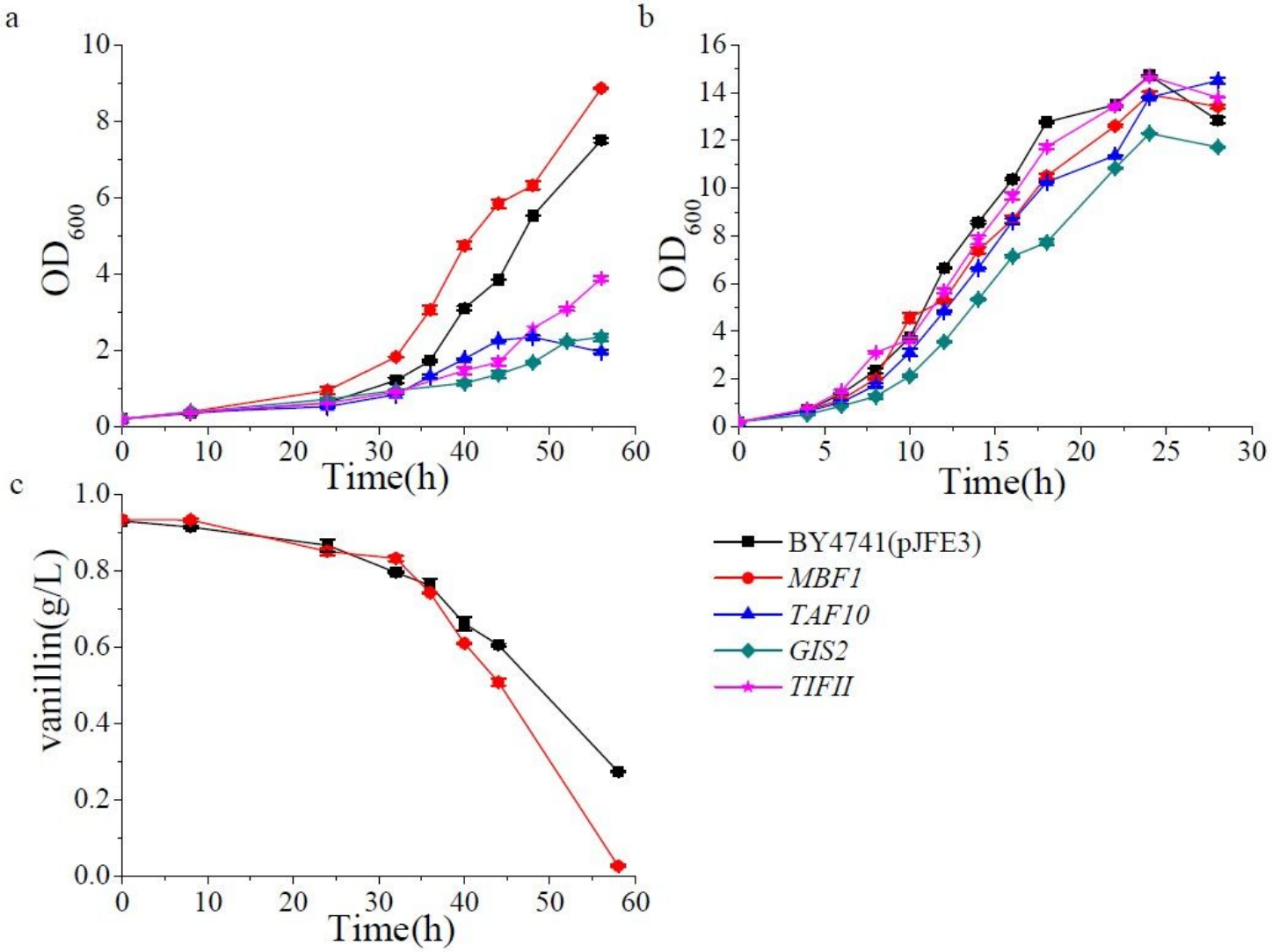

Figure 4

Vanillin resistance profiles of recombinant strains in Sc-URA liquid medium. The curve of growth under 6 mM vanillin stress (a) and without vanillin stress (b); the curve of vanillin reduction (c); BY4741(pJFE3) is the control. The error bars indicated the standard deviation of independent triplicates.